



Mechanical properties of glass fibre composites based on nitrile rubber toughened modified epoxy resin[☆]

M.R. Ricciardi^a, I. Papa^{b, *}, A. Langella^b, T. Langella^b, V. Lopresto^b, V. Antonucci^a

^a Institute for Polymer, Composites and Biomaterials, National Research Council, Piazzale Enrico Fermi, 1, 80055 Portici, Italy

^b Department of Chemical, Materials Engineering and Industrial Production, University of Naples Federico II, Piazzale Vincenzo Tecchio 80, 80125 Naples, Italy

ARTICLE INFO

Keywords:

Rubber
Composites
Mechanical properties
Shear
Impact

ABSTRACT

The aim to improve the impact behaviour of composite laminates and to reduce the problem of the complex damages after dynamic loads, a two-component commercial epoxy resin was modified with a commercial nitrile liquid rubber modified DGEBA epoxy prepolymer that, prior the cure, has been mechanically dispersed at two concentration levels (20%w/w; 30%w/w). Experimental characterization of both neat and modified resins was performed to investigate the effect of the rubber addition on the resin properties, i.e. glass transition temperature, modulus and dynamic mechanical characteristics. Further, the rubber domain distribution in the epoxy resin was analyzed by scanning electron microscopy (SEM). The hybrid rubber modified resins did not show high viscosity allowing to manufacture E-glass fiber reinforced composites by vacuum infusion process.

The laminates were characterized by tensile mechanical tests that evidenced an overall enhancement of maximum stress and deformation for the hybrid composites. In particular, results demonstrated an improvement of 10% for the shear failure stress and of 110% for the shear failure strain. Further, impact tests were carried out at penetration, to evaluate the improvement of the impact resistance over the conventional epoxy resin system, and at increasing energy levels, 5 J, 10 J and 20 J, to investigate the damage start and propagation. A higher indentation has been observed for the modified composite samples related with a lower delamination extension.

1. Introduction

Epoxy resins are the most common thermosetting materials for the manufacturing of fiber reinforced composite materials due to their good chemical and thermal resistance. The latter allow several engineering applications in many fields, such as automotive, aeronautic, electric, civil and electronic. However, some applications are limited by their crack resistance and inherent brittleness, depending on their highly crosslinked network not able to absorb energy during impact or fracture. Thus, several investigations [1–4] have been performed with the aim to improve the toughening properties of epoxy resins. The most successful method involves the mixing of the epoxy resin with low-molecular weight liquid rubbers prior the curing stage. The addition of liquid rubber materials provides a consolidated system with a two-phase microstructure [5] with enhanced toughness and a decrease

in modulus and glass transition temperature. The toughening effect of rubber on brittle polymers mainly depends on cavitation on the particles, controlling the shear yielding in the matrix and particles deformation [6], that enable the crack bridging due to their large extension [7]. More recently, some authors [8–10] investigated the use of core shell nano rubbers, such as polysiloxane [9] and butadiene/styrene [10] nanoparticles: they found a higher efficiency of nanometer particles as tougheners, compared to the submicron rubber particles, and the importance to use a reactive diluent for the epoxy resin [8].

Some authors have also studied the influence of rubber addition on the mechanical behaviour and fracture toughness of fiber-reinforced composites with epoxy matrix [5,11,12] even if, in this case, processing issues need to be overcome. In fact, addition of rubber can increase the viscosity of the resin making difficult the fiber impregnation. Further, in the case of infusion technology filtering of rubber additives can

[☆] The results of this work have been presented at the International Symposium on Dynamic Response and Failure of Composite Materials, DraF2016, Ischia, Naples, 6–9 September 2016.

* Corresponding author.

Email address: ilaria.papa@unina.it (I. Papa)

occur inducing a not homogenous distribution of rubber and only a partial transfer of hybrid resin properties to the final composite [13].

Given the non homogeneous and anisotropic nature of composite materials, they usually suffer hardly detectable damage under dynamic loads [14,16]. In the presence of through thickness stresses, the damage can propagate, often catastrophically, and lead the structural systems to final failures. The impact response of composite laminates and structures is a very complex process, which involves stress wave transfer, damage initiation, propagation and interaction, heat and sound transfer, phase changes and other complex mechanisms; the multiple damage mechanics typically interact with each other and lead to a considerable reduction of stiffness and strength in critical areas and, consequently, to the reduction of the load-carrying capability of the entire structure [16–18].

Despite the wide investigations performed over the years by the scientific community [19–21], the behaviour of composite materials and structures under low velocity impact is not completely understood yet.

However, the first damage that occurs in impact conditions was found to be cracks in the matrix that propagate up to reach the fibre-matrix interface, causing delamination [19,20,23,24]. Since the importance of the matrix type, good results have been achieved by increasing the toughness of the matrix by the addition of liquid rubber [26,27,35,37] or thermoplastic particles [28,29].

Nash et al. [25] give an extensive overview of different methods to improve the impact and post-impact performance of carbon fibre-reinforced composites (CFRP). The mechanisms of energy absorption, involving both fibre and matrix, as well as the fibre-matrix interaction, play a fundamental role [19,30,31,33,34,36].

In this study, a two-component commercial epoxy resin (ISX-10 by Mates Italiana) has been modified by dispersing a nitrile liquid rubber (STRUKTOL® POLYDIS® 3605) prior the cure at two concentration levels (20%w/w; 30%w/w) at the main aim to improve the dynamic response of polymeric composite laminates in terms of impact damage reduction. Experimental characterization of both neat and modified resins has been performed to investigate the effect of the rubber addition on the resin properties, i.e. glass transition temperature, modulus and dynamic mechanical characteristics. Further, scanning electron microscopy (SEM) has been used to verify the rubber domain distribution in the epoxy resin. Very interestingly, the hybrid rubber modified resins did not show high viscosity allowing to manufacture E-glass fiber reinforced composites by vacuum infusion process. Hence, composites, based on the neat and 30% w/w rubber modified resin, were realized and characterized by tensile mechanical tests evidencing, in particular, an overall enhancement of shear properties. Further, to test the improvement of the impact resistance over the conventional epoxy resin system, impact tests were carried out at penetration and at increasing energy levels, 5 J, 10 J and 20 J, to investigate the damage start and propagation.

The results showed a deeper indentation measured on the modified 30% w/w rubber sample but related to a lower delamination extension. The result is very interesting not only because of the internal damage reduction, but also for security reasons: a less important non visible damage corresponds, in fact, to a more evident external and so, visible, sign. It gives the opportunity to certainly know about the presence of delamination.

2. Experimental

2.1. Materials

The investigated system was a commercial two component liquid epoxy resin ISX_10 (by Mates Italiana) that was properly modified with Struktol Polydis 3605, a commercial nitrile liquid rubber modified DGEBA epoxy prepolymer supplied by Struktol, having a nitrile-butadi-

ene rubber content of 35% and viscosity at 25 °C of 50 Pa s. Unidirectional E glass fibers with 300gr/m² by Hexcel have been used as reinforcing elements for the manufacturing of composites. The resin system was modified by dispersing the rubber at 20% w/w and 30%w/w.

2.2. Fabrication methods

2.2.1. Polymer

Samples containing 0, 20% w/w and 30% w/w of nitrile liquid rubber were prepared and named respectively: neat, N20 and N30. Table 1 shows the formulation of the three investigated resin systems that were realized by mechanical mixing with a homogenization cycle for 15 min and a homogenization speed of 9600 rev/min (TURRA TURRAX 18 basic (IKA, Staufen, Germany).

After mixing and hardener addition, the resin systems were cured in the oven for 50 min at 90 °C.

2.2.2. Composite laminates

Fiber reinforced composites based on the neat and N30 resin have been manufactured by vacuum infusion process technology. The fibrous reinforcement was laid onto an open-faced heating plate. After stacking a peel ply and a bleeder material, a resin distribution medium (Green net) was placed on the top and partially in contact with the heating plate, useful for helping the resin to impregnate all plies. One nylon vacuum bag was put on the layers to cover the entire plate and stitched to the plate. After infusion, the panels were cured for 50 min at 90 °C.

2.3. Testing techniques

2.3.1. Differential scanning calorimeter (DSC) on polymer

Dynamic differential Scanning Calorimetry tests were performed by TA-Q1000 (TA Instruments Ltd, West Sussex, UK) at 10 °C/min from –80 °C up to 250 °C, followed by cooling to –50 °C.

2.3.2. Dynamic mechanical analysis (DMA) on polymer

Mechanical tests were performed by a TA-DMA Q800 equipped with single cantilever clamp and nominal sample size of 17.5 × 12.75 × 3.15 mm. The analysis was carried out from 30 to 200 °C at heating rate of 3 °C/min by using a constant frequency strain (1 Hz).

2.3.3. Morphology analysis (SEM) on polymer

The morphology and fracture surface of the resins were studied by using Esem_Fei_Inspect_S, Electron microscope coupled with Oxford INCA PentaFETx3 EDX spectrometer, which is a Si(Li) detector, nitrogen cooled and equipped with an ultrathin window ATW2. The results were, then, processed by an INCA software energy.

2.3.4. Static mechanical properties of composite laminates

The In-Plane Shear and the static 0° and 90° tests were carried out following the ASTM D 3518/D 3518M and D3039/D3039M – 14 STANDARD respectively by the test machine MTS 810 and with a test speed of 2 mm/min.

Table 1
Formulation of investigated resin systems.

Sample	Epoxy (g)	Hardener (g)	Nitrile rubber (g)
N	75	25	
N20	56	24	20
N30	49	21	30

2.4. Impact properties of composite laminates

Impact tests were carried out by a falling weight machine, Ceast Fractovis, at complete penetration, to obtain and study the whole load curve, interesting for giving useful information about the response of the laminates and for investigating the effect of the varied parameters. Then different increasing energy levels, 5 J, 10 J and 20 J, were chosen to carry out the so called indentation tests, useful to study the damage start and evolution. The rectangular specimens, 100 × 150 mm, cut by a diamond saw from the original panels, were supported by the clamping device suggested by the ASTM D7137 Standard and were centrally loaded by an instrumented cylindrical impactor with a hemispherical nose, 19.8 mm in diameter. The total minimum mass of 3.640 kg, that combined with the drop heights allowed to obtain the selected impact energies, was considered. After the impact tests, thanks to the transparency of the glass fibres, the specimens were observed by visual inspection to investigate the internal damage, whereas a confocal microscope, Leica DCM3D, was used to measure the indentation depth.

3. Results and discussion

3.1. Polymer

Differential scanning calorimeters and dynamic mechanical analyzer tests have been used to determine the fundamental properties of the investigated resin systems: the glass transition temperature T_g and the loss and storage modulus. The reported results have been obtained by averaging over three tests.

Table 2
DSC and DMA glass transition temperatures for investigated resin systems.

Sample	T_g , °C (DSC)	T_g , °C (DMA)
N	88	88
N20	72	78
N30	68	72

Table 2 shows the T_g values as obtained from DSC thermograms and the maximum of the $\tan \delta$ DMA curve.

The addition of liquid rubber causes a decrease in the glass transition temperature. In particular, from DSC results it can be observed that the T_g falls from 88 °C for the neat epoxy resin to 72 °C for 20% w/w liquid rubber modified epoxy resin and 68 °C for 30% w/w liquid rubber modified epoxy resin. This decrease in T_g can be related to the lower network density of the rubber based epoxy resins. In fact, when an epoxy resin, modified by rubber additives, cures, the rubber phase forms a secondary phase, the rubber domains. Some of rubber molecules do not participate to the phase separation, but crosslink in random way by lowering the network density.

The dynamic mechanical analyzer was used also evaluate the loss and storage modulus as a function of rubber addition to the epoxy resin. Fig. 1 show the average DMA data over three repeated tests in terms of the storage and loss modulus profile of the neat epoxy and modified epoxies. To prove the good repeatability of the data, Fig. 3 reports both the single test curves and the averaged one for N30 resin system. The storage modulus E' represents the stiffness of a viscoelastic material and it is proportional to the energy stored during a load cycle. As expected, this modulus decreases as the amount of rubber increases in the epoxy matrix, that results less stiff (see Fig. 2).

In particular, at 40 °C E' of neat epoxy is around 2 GPa, for 20% rubber resin is around 1.6 GPa while for 30% rubber resin is around 1.4 GPa. In all the cases, the values of E' decreased as temperature increases, indicating a change of state.

From the loss modulus curve it was observed that neat epoxy showed the highest T_g which means that the viscous dissipation was minimum for the epoxy resin. The addition of the rubber decreases the T_g temperature of epoxy phase and this also reflected in the epoxy $\tan \delta$ transition peak (Table 2). The decrease in T_g was due to the decrease in crosslink density of the cured resins. In fact, the liquid rubber can hinder the curing reaction of epoxy resin due to phase separation. Some of the partially cured epoxy resin may be trapped in the liquid rubber phase during the separation phase leading to incomplete curing. In fact, by comparing the cure reaction heat of N30 sample and that of the neat resin, the cure conversion of N30 sample was 15% less than that of neat. Thus, the crosslink density decreases resulting in a decrease in the T_g of the epoxy rich phase.

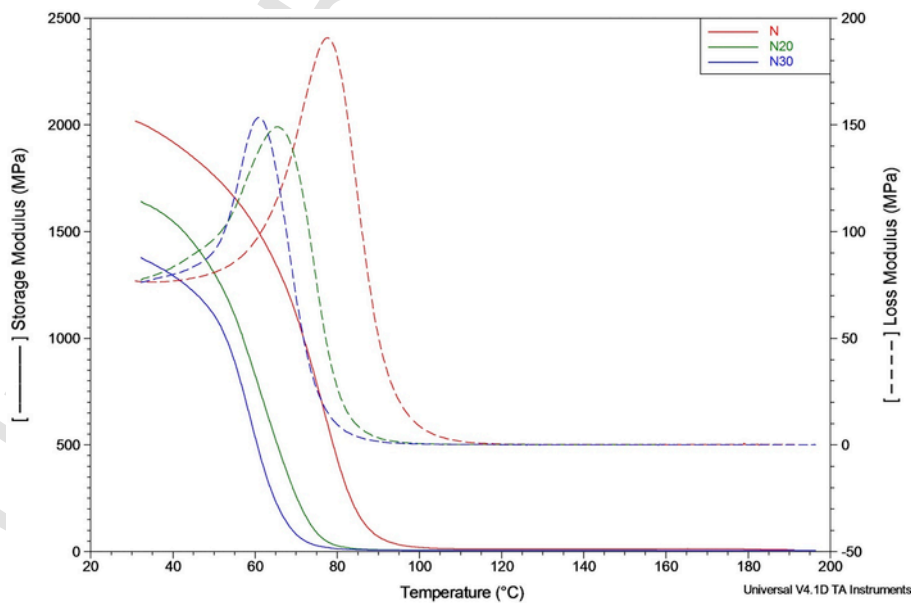


Fig. 1. Storage and loss modulus versus temperature of the neat epoxy and modified epoxies.

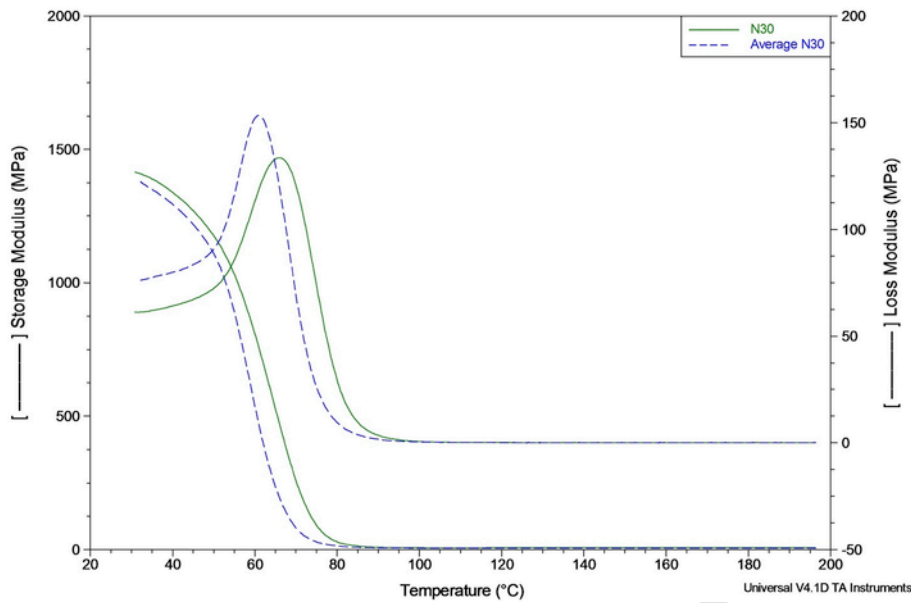


Fig. 2. Storage and loss modulus versus temperature of N30 modified epoxies.

The scanning electron microscopy has been used to investigate the morphology of the investigated resins. The micrographs were taken by the samples obtained after DMA tests. Fig. 3 shows the fracture surface of the neat epoxy samples. A smooth glassy fracture surface with cracks in different planes can be observed denoting a brittle behaviour without plastic deformation.

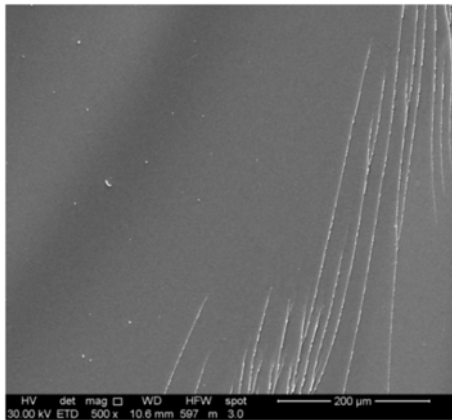


Fig. 3. SEM micrograph of neat epoxy.

The fractured surface of N20 and N30 rubber modified epoxy resin samples is shown in Figs. 4 and 5 respectively with a different level of magnification.

According to the literature, a two phase morphology with a continuous rigid phase and a dispersed rubber phase of isolated spherical particles is displayed. Thus, the toughness and the shear properties of rubber based resins should be enhanced by the presence of soft rubber particles that do not participate to the cure reaction and precipitate out from the reacting mixture. When a shear stress is applied to the hybrid system, a greater resistance is expected because the flexible spherical particles act as stress concentrator points and provide a plastic deformation behaviour and a greater capability to sustain the shear stress. In addition, the particles size increases as the rubber content increases.

SEM analysis has been performed also on fiber reinforced composite based on N30 rubber resin. Fig. 6 shows the fractured surface; in particular Fig. 6a and b are relative to the composite fibers, while 6c to the matrix area. A good adhesion can be observed between the glass fiber and the polymeric matrix. In addition, the rubber particles are distributed on the fiber surface and dispersed within the polymer matrix, creating a sort of flexible interphase.

Thus, due to homogenous dispersion of the rubber and no significant rheological differences between the N20 and N30 resin systems, the mechanical and impact tests have been performed for the neat and

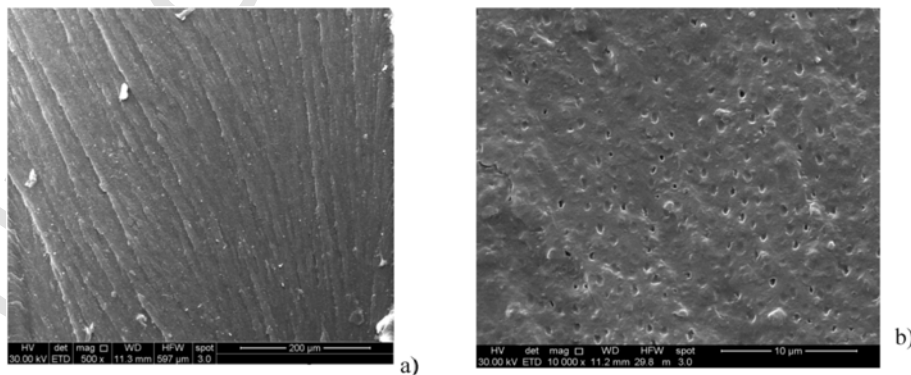


Fig. 4. a) SEM micrograph of N20 resin; b) Magnified micrograph of N20 resin.

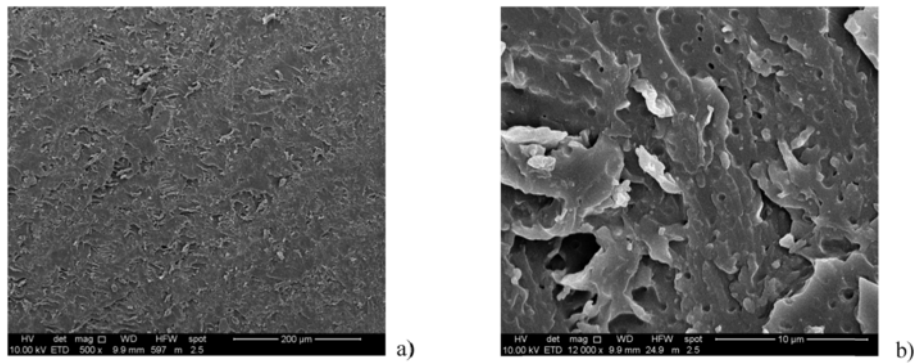


Fig. 5. a) SEM micrograph of N30 resin; b) Magnified micrograph of N30 resin.

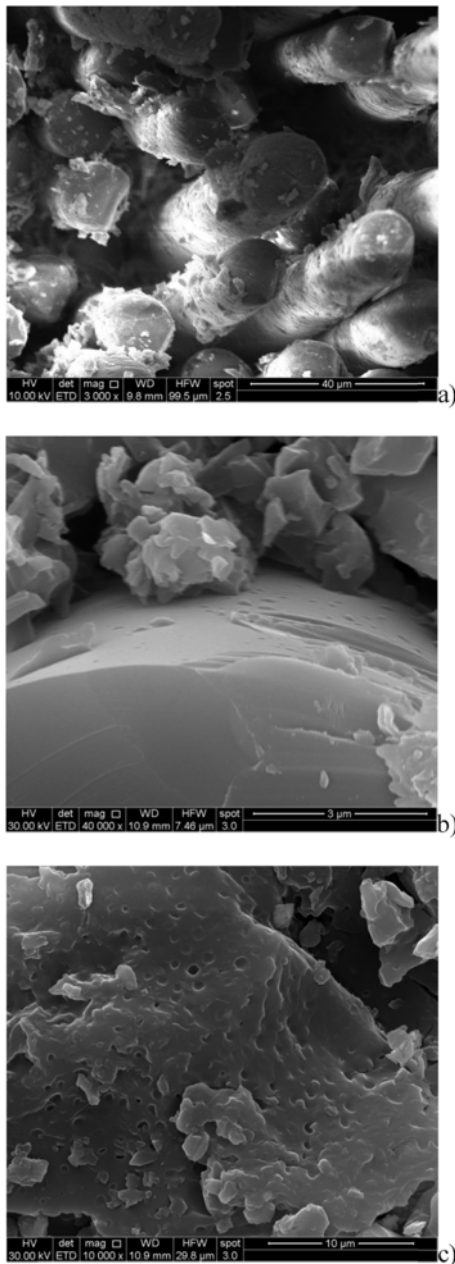


Fig. 6. a) SEM micrograph of N30 fibre reinforced composite b) Magnified micrograph of N30 resin on a fiber c) SEM micrograph of N30 resin within the composite.

N30 rubber resin composites in order to investigate the maximum toughness effect of the rubber addition on the composite performance.

4. Mechanical properties

4.1. Composites

Fig. 7 shows the obtained stress–strain curves for all studied polymeric composite systems during the tensile and shear tests.

The curves present slight different slopes that rely on different moduli. Both the neat and the modified laminates are characterized by linear behaviour until crack initiation indicated by the elbow of the curve. After that, as the strain increases, the laminate reaches a steady-state behaviour and, after a maximum value of the load, the sudden drop load happens corresponding to the samples break.

In Tables 3 and 4, the tensile and shear properties obtained by averaging the results of five tests were reported.

The reduction of the strength, σ , due to the modified resin R30 (Table 3), may be attributed to the lowering in crosslinking density of this polymeric system. No important differences were recorded among the mechanical properties.

To highlight the effect of loading of rubber on the mechanical behaviour of the tested samples, the data presented in Tables 3 and 4 are reported in Figs. 8 and 9 in a bar graphs. It gives a general overview of the influence of the modifier and the loading direction respect to the fibers, on modulus, E , strength, σ , and maximum elongation, ϵ . The laminates made by the addition of the rubber resin modifier, showed similar mechanical properties in all the tested directions ($0^\circ, 90^\circ, 45^\circ$), due to the important role of the fibres. Furthermore, in the shear plane (45°), the modified samples show a high elongation value at the final failure that resulted 210% greater than that of the neat one. The result is due to the more toughened behaviour of the rubber resin interested by this load.

5. Impact properties

Fig. 10 compares the contact force-deflection curves for GFRP laminates during each experimental low velocity impact tests up to penetration. The neat composite is indicated with the suffix R, the hybrid one with the addition of 30% of rubber, is labelled with the suffix R30. Clearly, the structural rigidity, represented by the initial slope of curves, increases with the nitrile rubber addition. No delamination effect or fiber failures, seem to occur since no load drops or changing in slope are evidenced by the curve. The maximum force decreases as the epoxy modifier percentage increases.

Impact penetration parameters as load peak (F_{max}), Energy at load peak (Energy), time at load peak, deflection at load peak and the pene-

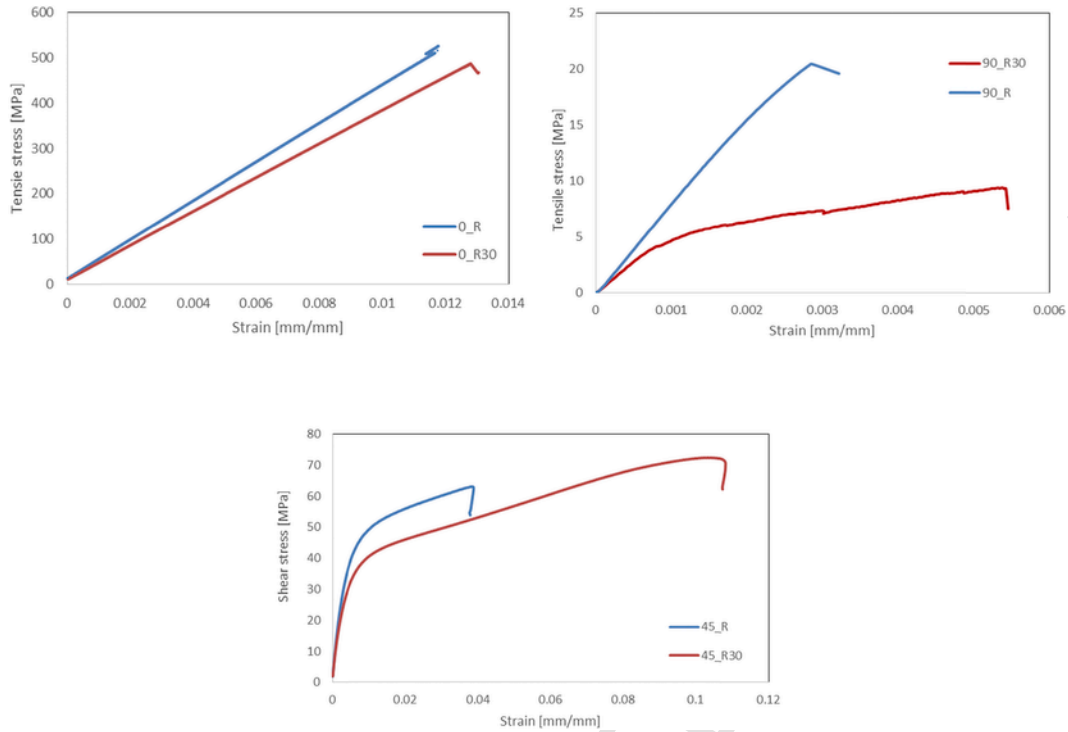


Fig. 7. Stress load versus strain for all tested direction: (a) 0°; (b) 90°; (c) 45°.

Table 3
Tensile properties 0°/90° of the neat and modified composites (ASTM D3039).

Sample	0°					90°				
	ϵ_1	σ_1 [MPa]	E1 [MPa]	Dev ϵ_1	Dev σ_1	ϵ_2	σ_2 [MPa]	E2 [MPa]	Dev ϵ_2	Dev σ_2
R	0.0125	537.18	42911	0.0002	8.9416	0.006	25.42	7455	0.0011	0.5970
R30	0.0139	502.60	36536	0.0006	6.2437	0.008	11.22	5675	0.0064	3.3141

Table 4
Shear properties $\pm 45^\circ$ of the neat and modified composites (ASTM D3518).

Sample	ϵ	τ [MPa]	E [MPa]	Dev ϵ	Dev τ
R	0.039	66.52	6917	0.0202	3.0616
R30	0.121	72.76	3476	0.0341	1.8264

tration energy (U_p), measured on the load curve at penetration, are reported in Table 5.

In Fig. 11, Fig. 12 and Fig. 13 typical load-deflection curves for the different samples impacted at the different energy levels of 5, 10 and 20 J, are reported for the all the specimens tested.

The graph clearly shows that, closed type curves are obtained at the different conditions: the samples are not penetrated/perforated by the impactor that rebounds, and the area enclosed in the loop of the loading and unloading part of the curve, represents the energy absorbed by the laminate to create damage. As clear, no significant differences were observed between the neat and hybrid laminates except a slight lower-

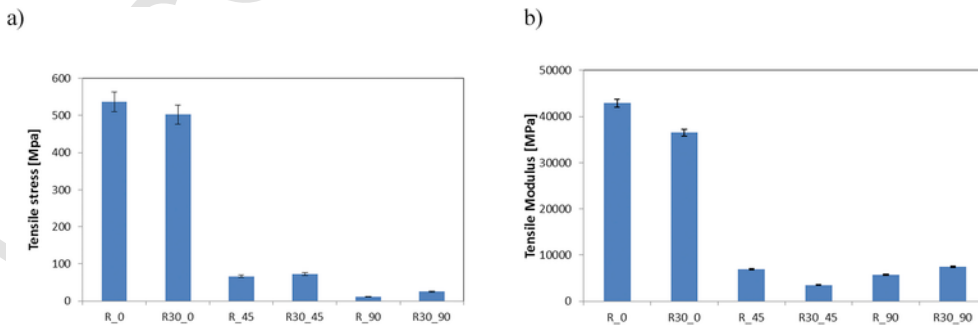


Fig. 8. Tensile tests: stress (a) and modulus (b).

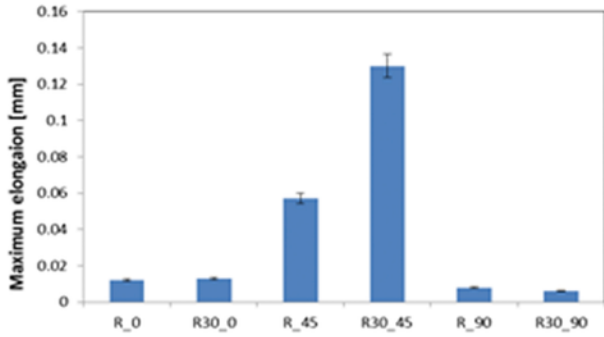


Fig. 9. Tensile tests: maximum elongation.

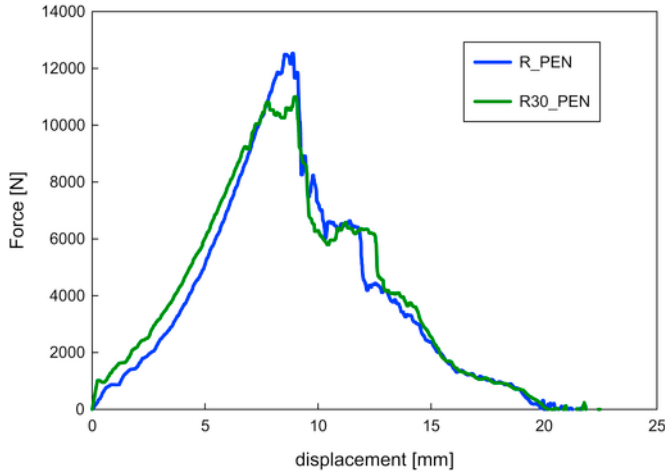


Fig. 10. Force-displacement penetration curves (R:neat; R30: 30%wt).

Table 5
Low velocity impact penetration data.

Type	Properties at maximum load					U_p (J)
	$F_{max}(N)$	Energy (J)	time (ms)	Displacement (mm)		
R	12521	46	2.70	8.85		85
R30	11002	51	3.44	9.02		89

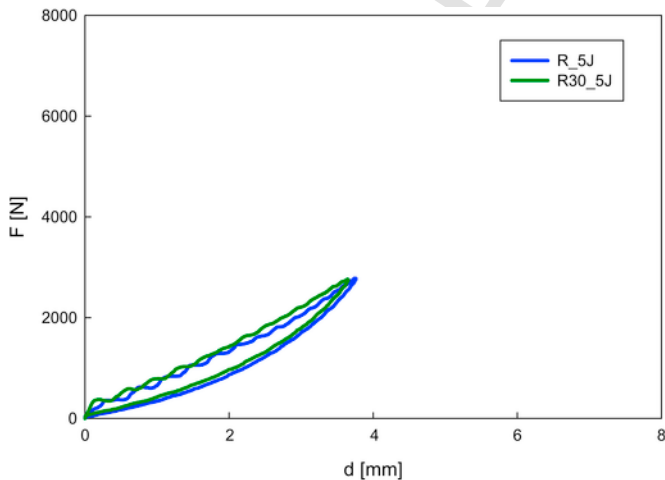


Fig. 11. Force - deflection curves of reinforced composites (5 J) (R:neat; R30: 30%wt).

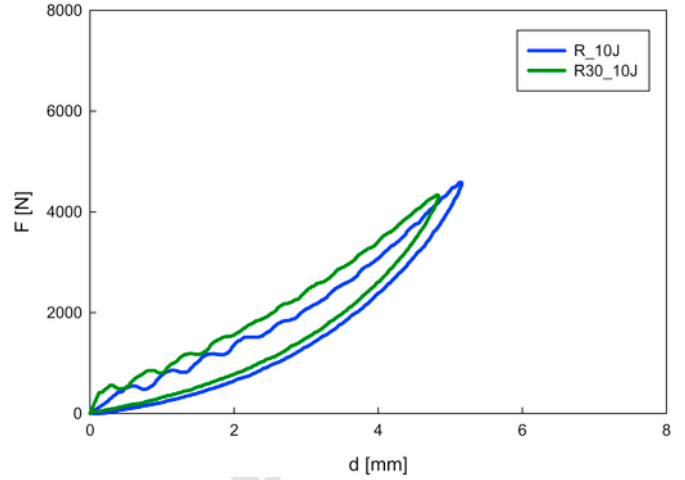


Fig. 12. Force - deflection curves of reinforced composites (10 J) (R:neat; R30: 30%wt).

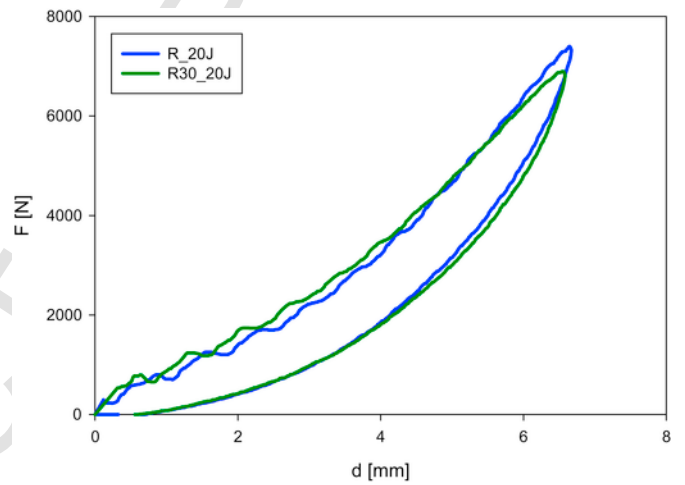


Fig. 13. Force - deflection curves of reinforced composites (20 J) (R:neat; R30: 30%wt).

ing of the curve for the laminate with 30 wt% of modifier, observed at high deflection values (Fig. 13).

As expected, the maximum impact load, F_{max} , increases at the increasing of the impact energy, U_p , (Fig. 14). Also the absorbed energy, U_a , increases at the increasing of the impact energy, U_p , meaning that the effect of the increasing energy is like the increasing in rigidity that causes an increase in internal damage. To confirm what asserted, the damaged area, A , was correlated (Fig. 16) to the impact energy, U : a linear relationship was observed in the range of the adopted impact energy.

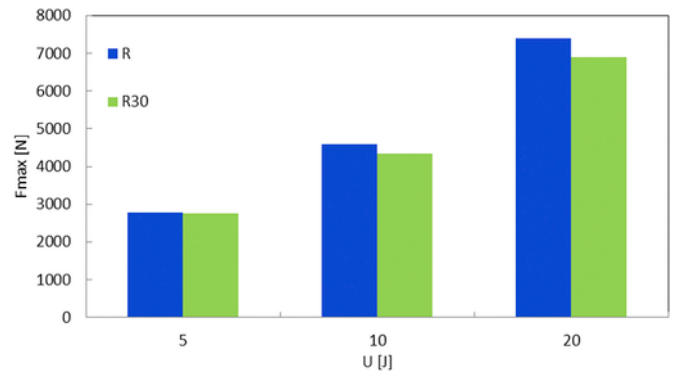


Fig. 14. Maximum impact load-impact energies for composites (R:neat; R30: 30%wt).

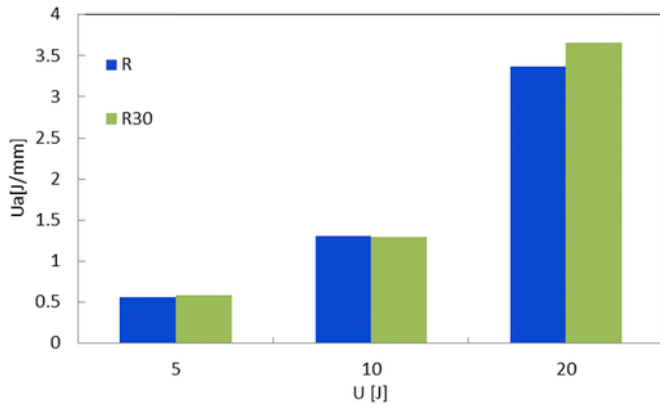


Fig. 15. Absorbed energy, U_a , versus impact energy, U (R: neat; R30: 30%wt).

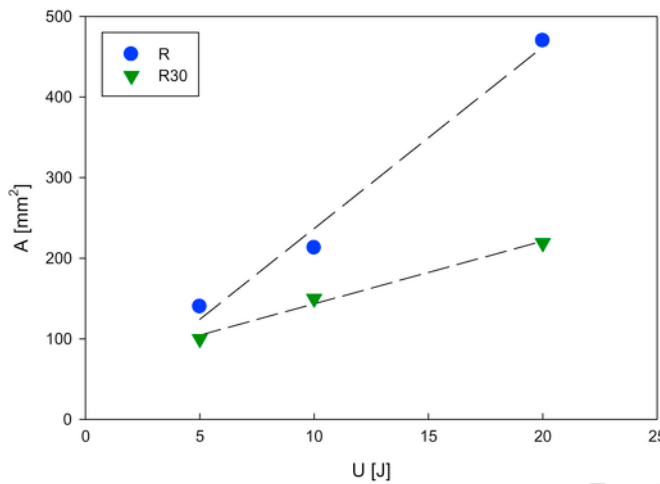


Fig. 16. Delaminated area, A , versus impact energy, U .

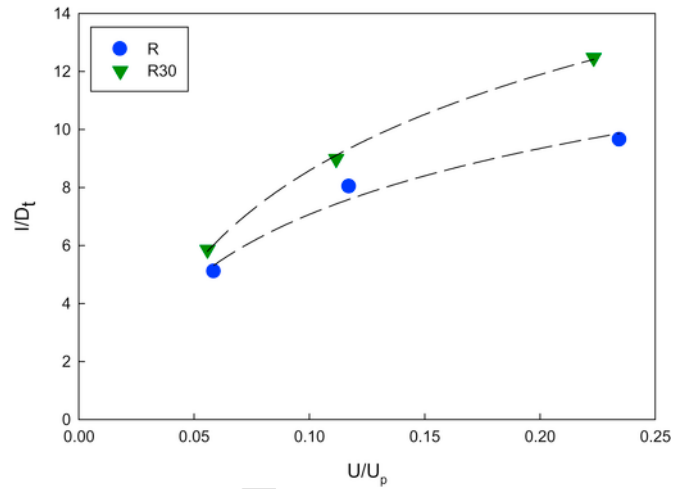


Fig. 17. Indentation depth, I/D_t , versus impact Energy, U/U_p .

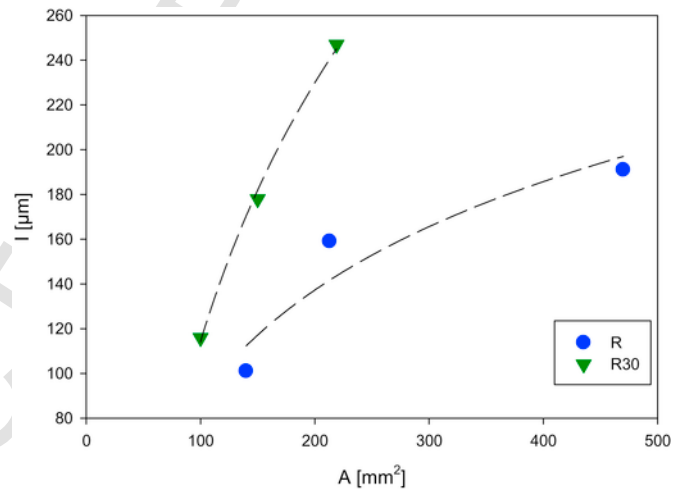


Fig. 18. Indentation depth, I , versus delaminated area, A .

ergies. By a comparison at a fixed impact energy, the delaminated area was found to be lower in the panels modified by a rubber percentage of 30% by weight of the resin respect. However, this result is not reflected by the trend of the absorbed energy, U_a , versus the impact energy, U (Fig. 15) and it could mean that, for a fixed absorbed energy, it is more difficult the damage propagation when the resin is modified by the nitril rubber.

In Fig. 17, the ratio between the indentation depth, I , the plastic deformation left by the indenter on the surface of the impacted laminate, and the penetrator tip diameter, D_t , was plotted against the non dimensional energy, U/U_p . An increasing of I/D_t at the increasing of U/U_p was noted. The increasing trend is lower, the higher is the U/U_p ratio and tends to a horizontal asymptote showing deeper depths on the modified laminates. It means that adding the rubber causes a more plastic behaviour, as confirmed also by the DSC and DMA analysis and the presence of the asymptote means that after a certain value of the impact energy, a part of the latter is absorbed to create damage mechanisms different from indentation. The effect of the minimum change of the panels thickness on the indentation was eliminated by considering the ratio between the impact energy, U , and the perforation one, U_p [32]. Plotting the indentation depth, I , against the delaminated area, A , (Fig. 18), by comparing the two different laminates, at a fixed delamination extension, a higher indentation value of the modified resin corresponds. The result represents an advantage since the same internal extension of the damage is externally evidenced by a more evident and clear signal.

6. Conclusions

The main physical properties, glass transition temperature, loss and storage moduli, of a commercial epoxy resin modified by addition of a nitrile liquid rubber have been investigated finding. A decrease of T_g and of storage modulus due to lower crosslink density of rubber based resin was found.

Glass fiber composite laminates in epoxy resin with a 30% wt. content of a nitrile rubber modifier were manufactured by vacuum infusion technology. Static and dynamic mechanical behaviour have been investigated.

6.1. The results revealed that

- In the shear plane (45°) respect to the fibre direction, the modified samples showed a higher elongation than the neat one up to the final crack.
- A reduction of the fracture stress, σ_f , obtained for the modified resin N30 is registered. It may be attributed to the lowering in crosslinking density of this polymeric system;
- During the penetration tests, a slight lowering of the curve for the laminate with 30 wt% of modifier has been noticed, in particular at $U = 20$ J;

- A linear relationship of the delaminated area, A , versus the impact energy, U , was obtained. The modified samples delaminated area resulted lower than the neat one even if the absorbed energy results the same in each case;
- Very interestingly, the modified composites showed smaller delamination even though the absorbed energy is the same and the load is higher. It means that the addition of the nitril rubber results in a more difficult damage propagation.
- The smaller delamination was signalled by a deeper indentation.

Uncited references

[15]; [22].

Acknowledgements

The authors gratefully acknowledge the ONR Solid Mechanics Program, in the person of Dr. Yapa D.S. Rajapakse, Program Manager, for the financial support provided to this research.

The authors want to specially thank Phd. Carla Velotti for the interesting discussion and for helping the authors in measuring the indentation depth.

References

- [1] R. Thomas, S. Durix, Christophe Sinturel, Tolib Omonov, Sara Goossens, Gabriel Groeninckx, et al., Cure kinetics, morphology and miscibility of modified DGEBA-based epoxy resin – effects of a liquid rubber inclusion, *Polymer* 48 (6) (8 March 2007) 1695–1710.
- [2] N.G. Ozdemir, T. Zhang, I. Aspin, F. Scarpa, H. Hadavinia, Y. Song, Toughening of carbon fibre reinforced polymer composites with rubber nanoparticles for advanced industrial applications, *eXPRESS Polym Lett* 10 (5) (2016) 394–407.
- [3] Lina Dong, Wenyang Zhou, Xuezheng Sui, Zijun Wang, Peng Wu, Jing Zuo, Huiwu Cai and Xiangrong Liu, Thermal, mechanical, and dielectric properties of epoxy resin modified using carboxyl-terminated polybutadiene liquid rubber, *J Elastomers Plastics* 1–17, DOI: 10.1177/0095244316653261.
- [4] Wenyang Zhou and Jing Zuo, Mechanical, thermal and electrical properties of epoxy modified with a reactive hydroxyl-terminated polystyrene-butadiene liquid rubber, *J Elastomers Plastics*, 32(18) 1359–1369.
- [5] L.L. Sobrinho, V.M.A. Calado, F.L. Bastian, Effects of Rubber Addition to an epoxy resin and its fiber glass composites, *Polym Compos* 295–305 (2012).
- [6] A.F. Yee, R.A. Pearson, *J Mat Sci* 21 (1986) 2462.
- [7] A.J. Kinloch, R.J. Young, *Fracture behavior of polymers*, Applied Science Publishers, London, 1983.
- [8] N.T. Kamar, L.T. Drzal, Micron and nanostructures rubber toughened epoxy: a direct comparison of mechanical, thermomechanical and fracture properties, *Polymer* 92 (2016) 114–124.
- [9] D. Carolan, A. Ivankovic, A.J. Kinloch, S. Sprenger, A.C. Taylor, Toughening of epoxy-based hybrid nanocomposites, *Polymer* 97 (2016) 179–190.
- [10] Feng Xu, Xu-Sheng Du, Hong-Yuan Liu, Wei-Guo Guo, Yiu-Wing Mai, Temperature effect on nanorubber toughening in epoxy and epoxy/carbon fiber laminated composites, *Compos part B* 95 (2016) 423–432.
- [11] D. Srinivasarao, M. Amareswari Reddy, M.N.V. Krishna Veni, M. Sandeep Kumar, Effect of nano rubber additions on wear and mechanical properties of epoxy glass fibre composites, *J Mater Sci Eng* 3 (2014) 143, <https://doi.org/10.4172/2169-0022.1000143>.
- [12] S. Sprenger, M.H. Kothmann, V. Altstaedt, Carbon fiber reinforced composites using an epoxy resin matrix modified with reactive liquid rubber and silica nanoparticles, *Compos Sci Technol* 105 (2014) 86–95.
- [13] S. Sprenger, Fiber reinforced composites based on epoxy resins modified with elastomers and surface modified silica nanoparticles, *J Mat Sci* 2391–2402 (2014).
- [14] B. Abdel-Magid, S. Ziaee, K. Gass, M. Schneider, *Compos Struct* 71 (2005) 326.
- [15] A. Khalid, *Mater Des* 27 (2006) 499.
- [16] S. Liu, Z. Kutlu, F.K. Chang, *J Compos Mater.* 27 (5) (1993) 436–470.
- [17] F.K. Chang, H.Y. Choi, H.S. Wang, 31st AIAA/ASME/ASCE/AHS/ASC structures, struct. Dyn. And mater. Conf., Long beach, CA, 1990930–940.
- [18] M.G. Stout, D.A. Koss, C. Liu, J. Idasetima, *Compos Sci Technol* 59 (1999) 2339–2350.
- [19] G. Caprino, V. Lopresto, C. Scarponi, G. Briotti, Influence of material thickness on the response of carbon-fabric/epoxy panels to low-velocity impact, *Compos Sci Technol* 59 (1999) 2279–2286.
- [20] F.K. Chang, H.Y. Choi, H.S. Wang, Damage of laminated composites due to low velocity impact, In: 31st AIAA/ASME/ASCE/AHS/ASC structures, struct. Dyn. And mater. Conf., Long Beach, CA, April 2-4, 1990, pp. 930–940.
- [21] A.J. Lesser, A.G. Filippov, Kinetics of damage mechanisms in laminated composites, *Int SAMPE Symp Exhib* 36 (1) (1991) 886–900.
- [22] E.F. Dost, L.B. Ilcewitz, W.B. Avery, in: T.K. O'Brien (Ed.), Effects of stacking sequence on impact damage resistance and residual strength for quasi-isotropic laminates, 1991, pp. 476–500, ASTM STP 1110.
- [23] H.Y. Choi, F.K. Chang, A model for predicting damage in graphite/epoxy laminated composites resulting from low-velocity point impact, *J Compos Mater.* 26 (14) (1992) 2134–2169.
- [24] S. Liu, Z. Kutlu, F.K. Chang, Matrix cracking and delamination propagation in laminated composites subjected to transversely concentrated loading, *J Compos Mater.* 27 (5) (1993) 436–470.
- [25] N.H. Nash, T.M. Young, P.T. McGrail, W.F. Stanley, Inclusion of a thermoplastic phase to improve impact and post-impact performance of carbon fibre reinforced thermosetting composites – a review, *Mater Des* 85 (2015) 582–597.
- [26] Z. Hengshi, X. Shiai, A new method to prepare rubber toughened epoxy with high modulus and high impact strength, *Mater Lett* 121 (2014) 238–240.
- [27] F.N. Nguyen, N. Natsume, N. Arai, K. Yoshioka, High performances of core-shell (dendrimer) nanoparticles in carbon fibre/epoxy composites, In: 18th International conference on composite materials (ICCM 18), Korea, 2011.
- [28] D.J. Bull, S.M. Spearing, I. Sinclair, L. Helfen, Three-dimensional assessment of low velocity impact damage in particle toughened composite laminates using micro-focus X-ray computed tomography and synchrotron radiation aluminography, *Compos A* 52 (2013) 62–69.
- [29] D.J. Bull, A.E. Scott, S.M. Spearing, I. Sinclair, The influence of toughening-particles in CFRPs on low velocity impact damage resistance performance, *Compos A* 58 (2014) 47–55.
- [30] G. Balaganesan, Vishwas Chandra Khan, Energy absorption of repaired composite laminates subjected to impact loading, *Compos Part B Eng* 98 (1) (August 2016) 39–48.
- [31] O. Dorival, P. Navarro, S. Marguet, C. Petiot, M. Bermudez, D. Mesnag e, et al., Experimental study of impact energy absorption by reinforced braided composite structures: dynamic crushing tests, *Compos Part B Eng* 78 (1) (September 2015) 244–255.
- [32] G. Caprino, V. Lopresto, The significance of indentation in the inspection of carbon fibre reinforced plastic panels damaged by low-velocity impact, *Compos Sci Technol* 60/7 (2000) 1003–1012.
- [33] A. Riccio, A. De Luca, G. Di Felice, F. Caputo, Modelling the simulation of impact induced damage onset and evolution in composites, *Compos Part B Eng* 66 (October 2014) 340–347.
- [34] A. Riccio, S. Saputo, A. Sellitto, A user defined material model for the simulation of impact induced damage in composite, *Key Eng Mater* 713 (2016) 14–17.
- [35] L. Vertuccio, L. Guadagno, G. Spinelli, S. Russo, G. Iannuzzo, Effect of carbon nanotube and functionalized liquid rubber on mechanical and electrical properties of epoxy adhesives for aircraft structures Original Research Article, *Compos Part B Eng* 129 (15) (November 2017) 1–10.
- [36] Veera M. Boddu, Matthew W. Brenner, Jignesh S. Patel, Ashok Kumar, P. Raju Mantena, Tezeswi Tadepalli, et al., Energy dissipation and high-strain rate dynamic response of E-glass fiber composites with anchored carbon nanotubes Original Research Article, *Compos Part B Eng* 88 (1) (March 2016) 44–54.
- [37] Nazli G. Ozdemir, Tao Zhang, Homayoun Hadavinia, Ian Aspin, Fabrizio Scarpa, Glass fibre reinforced polymer composites toughened with acrylonitrile butadiene nanorubber Original Research Article, *Compos Part B Eng* 88 (1) (March 2016) 182–188.